Reynolds Number Effects on Mixing and Combustion in a Reacting Shear Layer

M. G. Mungal,* J. C. Hermanson,† and P. E. Dimotakis‡
California Institute of Technology, Pasadena, California

The temperature field is investigated in a gaseous, reacting mixing layer formed between two streams containing low concentrations of hydrogen and fluorine, over a wide range of Reynolds numbers. The results show the presence of large, hot structures that govern the flow dynamics at all speeds. The mean-temperature profile is found to decrease modestly with increasing speed, a result suggesting a weak Reynolds number dependence of the production rate. Tripping the high-speed boundary layer is found to have a significant effect on the width of the mixing zone and the profile of the mean temperature rise.

Introduction

In this investigation the mixing and product formation of a two-dimensional shear layer was investigated, employing weak reactant concentrations of hydrogen and fluorine carried in separate inert, nitrogen freestreams. These reactants form hydrogen fluoride with release of heat which serves as a label of the molecularly mixed fluid. The heat release was kept low so that the overall properties of the mixing layer were not significantly changed from the cold, nonreacting case.

This work is a continuation of earlier work[18,19] and was aimed specifically at determining the effect, if any, of Reynolds number upon the entrainment, mixing, and combustion processes. The recent Broadwell-Breidenthal model[5] has suggested that Reynolds number may play a role similar to that of Schmidt number, and would manifest itself as a decreasing mean product (temperature) profile even in the limit of infinitely fast chemistry. In this model, the amount of product in the shear layer is decomposed into a Reynolds number and Schmidt number independent part, and, a Reynolds number and Schmidt number dependent part. This latter contribution to the total amount of product is such that increasing the Reynolds number leads to a decrease in the amount of product formed.

Experimental Apparatus

The experimental facility has been described previously[18,19] and will only be discussed briefly. It is of the blowdown type, in which premixed volumes of hydrogen in nitrogen and fluorine in nitrogen are discharged through sonic orifices, maintaining a constant mass flux in each of the shear layer freestreams. Both streams enter a settling and contraction section for turbulence reduction with the high-speed flow emerging from a 6:1 contraction with an exit area of 5×20 cm, and the low-speed flow emerging from a 4:1 contraction with a 7.5×20 cm exit area. The streams meet at the tip of a splitter plate shown in Fig. 1. All measurements are recorded at a station $x=45.7$ cm downstream of the splitter plate trailing edge.

Presented as Paper 84-0371 at the AIAA 22nd Aerospace Sciences Meeting, Reno, Nev., Jan. 9-12, 1984; received March 7, 1984; revision received Jan. 18, 1985.

*Research Fellow, Aeronautics. Member AIAA.
†Presently, Graduate Student, Aeronautics. Member AIAA.
‡Associate Professor, Aeronautics and Applied Physics. Member AIAA.

Runs were performed for flow velocities of $U_1=13.5$, 22.5, 44, and 85 m/s with a fixed speed ratio $U_2/U_1=0.40$. The Reynolds numbers corresponding to these conditions will be designated Re_1, Re_2, Re_3, and Re_4, respectively. By way of comparison, the earlier work[18,19] reported was performed at Re_2. The Reynolds numbers based on velocity difference and 1% thickness of the layer (points at which the mean temperature rise falls to 1% of the maximum mean temperature rise) are, respectively, 4.3×10^4, 6.7×10^4, 1.3×10^5, and 1.9×10^5 (based on velocity difference and downstream distance, the highest Reynolds number is 1.6×10^6). These values are all beyond the mixing transition observed by Konrad[16] and Breidenthal.[4] The high-speed turbulence level varied from about 1% rms at the lowest speed to about 0.3% rms at the highest speed.

Measurements

For each run the high-speed sidewall remained horizontal, while the streamwise pressure gradient was set to zero by adjustment of the low-speed sidewall. Temperature rise was recorded by a rake of eight cold wire resistance thermometers placed across the width of the layer, each driven by a constant current of 0.4 mA. A typical wire was made of 2.5-μm-diam platinum/10% rhodium welded to inconel prongs with a span of 1.5 mm. The ratio of the length of the wire to the cold length[20] is about 20 at Re_2. During a run, each wire was sampled at 7.5, 10, 12.5, and 15 kHz, for the four speeds, corresponding to total data rates of 60, 80, 100, and 120 kHz.

An important feature is the calibration procedure that was applied to each wire: prior to a run a small hot jet and a small cool jet, whose temperatures were accurately known, were applied to each probe in such a way that the entire wire and prong tips equilibrated to the jet temperature, and the probe voltages recorded. These two measurements thus provided the calibration constant to convert recorded voltage to temperature rise. During a run the hot flow performs a similar function to the hot jet, i.e., it brings the prong tips to a local mean temperature about which the wire performs excursions. Errors due to differences in the thermal conductivity of hot and cool regions of the flow were established to be small. The mean temperature is therefore accurate to within the calibration procedure, while excursions from the mean suffer from conduction error,[20] which can be as high as 10-20% for the wires used in these experiments. In any event, the mean-temperature profiles were spot checked by a 0.25-mm-diam chromel-alumel thermocouple at a single point on the mean temperature rise profile, with the agreement generally within 3% or better.

Flow visualization was accomplished by spark schlieren photography. A motor-driven, 35 mm camera was synchronized with a spark source (~3 μs duration) to produce approximately three photographs per second. A circular hole source mask and a circular hole spatial filter were used, instead of the conventional knife edge, in an effort to give equal weights to gradients of refractive index in all directions and to better resolve the large structures in the flow.

Chemistry

The chemical reaction utilized here is

$$H_2 + F_2 \rightarrow 2HF, \quad \Delta Q = -130 \text{ kcal/mole}$$

The heat release corresponds to a temperature rise of 165 K for 1% F_2 in N_2 and 8% H_2 in N_2 under constant pressure, adiabatic conditions (this is the so-called adiabatic flame temperature rise). The chemical reaction actually consists of two second-order chain reactions:

$$H_2 + F \rightarrow HF + H, \quad \Delta Q = -32 \text{ kcal/mole} \qquad (1)$$

$$H + F_2 \rightarrow HF + F, \quad \Delta Q = -98 \text{ kcal/mole} \qquad (2)$$

The first of these two reactions, referred to as the "cold" reaction, is about one order of magnitude faster than the second or "hot" reaction at room temperature.[8] Proper chain initiation requires some free F atoms and was accomplished in these experiments by premixing a trace amount of nitric oxide with the hydrogen carrying stream. The reaction

$$F_2 + NO \rightarrow NOF + F$$

was sufficient to provide the required F atom concentration in the layer to ensure proper ignition. For all runs reported here, the NO concentration was maintained at 3% of the freestream fluorine concentration. In any event, the flow is one in which the resulting chemical time scales are fast compared to the fluid mechanical time scales. The characteristic chemical time for the set of reactions was determined using the CHEMKIN chemical kinetics program.[15] At Re_2, the Damkohler number, which is the ratio of the mixing time to the chemical time, is about 10 for the local large scales (i.e., based on layer 1% thickness divided by the freestream velocity difference) or about 60 based on the time of flight to the measuring station (i.e., distance to measuring station divided by mean convection velocity). It is useful to note that Wallace,[22] who used nitric oxide and ozone as reactants, estimates Damkohler numbers that are similar to those reported here. For higher concentrations of reactants the Damkohler numbers will be higher,[12] while for increasing speeds the Damkohler number will become smaller. We do, however, believe that for all runs reported here, the chemistry is sufficiently fast so that the effects of slow chemistry are not an issue.

The equivalence ratio ϕ is defined here as the volume of high-speed fluid required to completely react with unit volume of low-speed fluid, or, as the ratio of the low-speed freestream molar concentration, c_{02}, to the high-speed freestream molar concentration, c_{01}, divided by the low-speed to high-speed stoichiometric ratio, i.e.,

$$\phi = \frac{c_{02}/c_{01}}{(c_{02}/c_{01})_s} = \frac{c_{02}}{c_{01}}$$

since the molar stoichiometric ratio for the hydrogen-fluorine reaction is unity. For all runs reported here, the high-speed stream consisted of 8%H_2, 92%N_2, and 0.03%NO, while the low-speed stream consisted of 0.96%F_2 and 99%N_2 (passivation of upstream screens and plates removed an estimated 0.04%F_2 from the nominal value of 1%F_2), with an adiabatic flame temperature rise of 159 K. This choice yields $\phi \sim 1/8$. It has been shown earlier[18,19] that choosing one stream to be eight times as concentrated as the other guarantees that the lean reactant is consumed to yield the asymptotic shape, for small ϕ, of the mean temperature profile (see also Ref. 22).

Results and Discussions

Part a of Figs. 2-5 shows the resulting time traces from the eight cold wires for an equivalence ratio of 1/8. The adiabatic flame temperature rise (labeled Tflm) for these flows is 159 K, and the time traces show the instantaneous temperature rise recorded by each probe as a function of time, normalized by the highest temperature rise seen by any probe during this time interval (labeled Tmax). The horizontal axis shows 512 points/probe and corresponds to 68, 51, 41, and 34 ms of real time for Re_1 to Re_4, respectively. Flow can be viewed as being from right to left, with the high-speed fluid on top. In addition, the time axis is greatly compressed: at Re_2, such a plot would be to scale if the horizontal distance were about nine times the distance between the high- and low-speed probes.

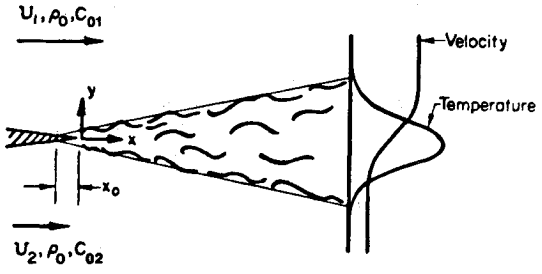

Fig. 1 Turbulent shear layer geometry.

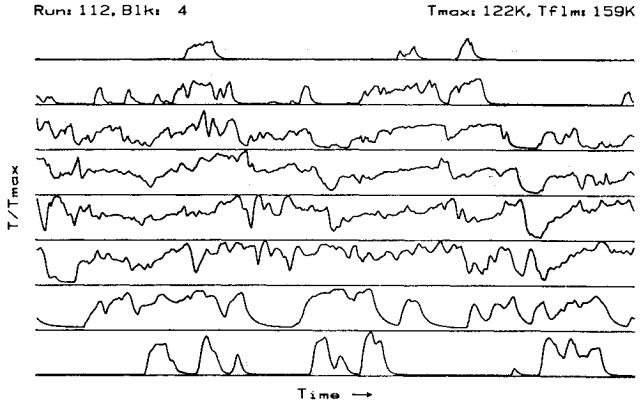

Fig. 2a Temperature vs time trace, Re_1.

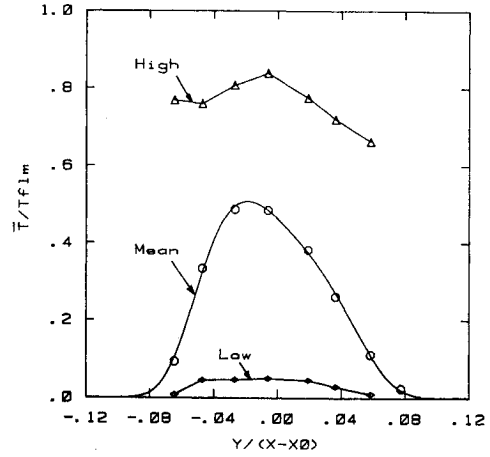

Fig. 2b Mean-temperature profile, Re_1.

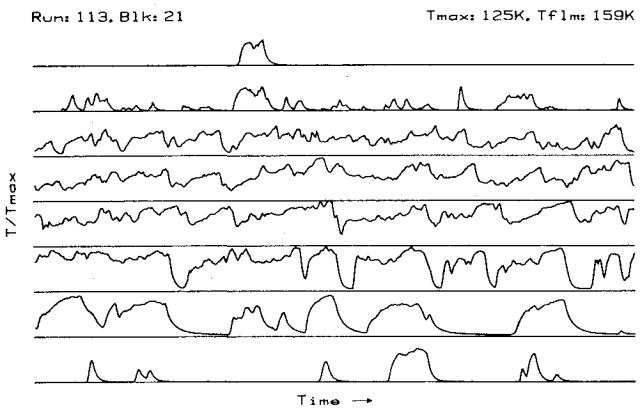

Fig. 3a Temperature vs time trace, Re_2.

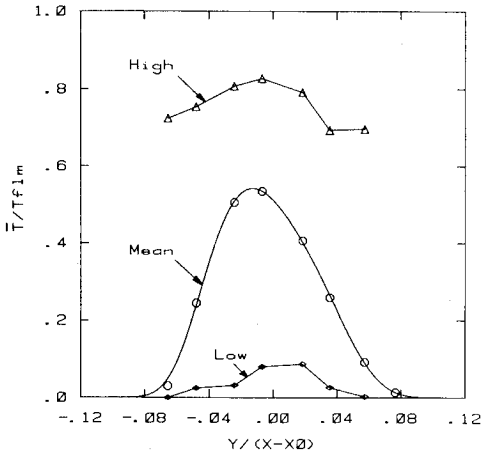

Fig. 3b Mean-temperature profile, Re_2.

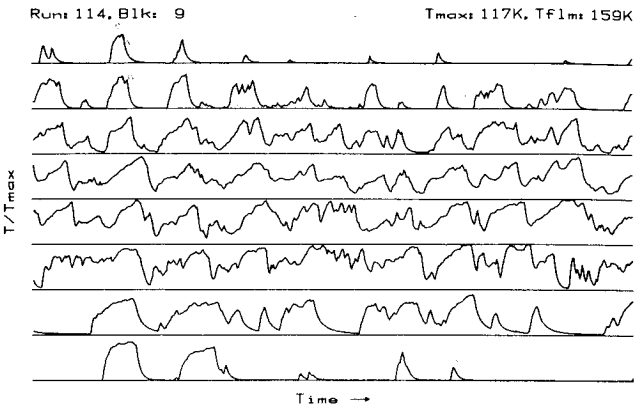

Fig. 4a Temperature vs time trace, Re_3.

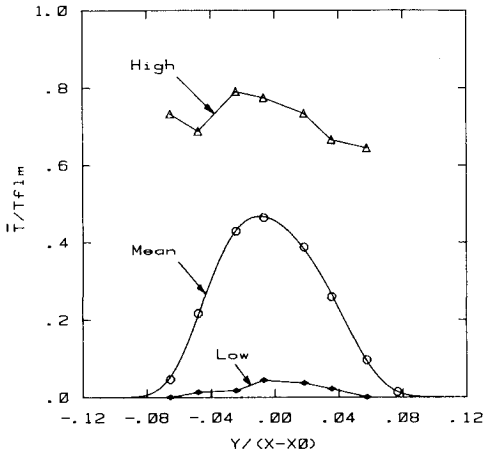

Fig. 4b Mean-temperature profile, Re_3.

The flow dynamics reported earlier[18,19] continue to be observed at these Reynolds numbers, namely: 1) the presence of large, hot regions or structures; 2) the presence of cool fluid tongues that extend well into the layer; and 3) the observation that within the core of the large structure, the temperature from one edge of the layer to the other is roughly uniform, i.e., the structure appears to be well mixed.[10] With respect to this final observation, it must be noted that the cold wires perform local averaging since they are unable to resolve the smallest scales in the flow. The dramatic thinning of the layer at Re_4 is associated with the fact that the high-speed boundary layer has tripped naturally, leading to a different growth rate.[1,6] Since the large structure spacing[2] is roughly 1.5 times the visual width of the layer, the corresponding structure passage times would be 12.0, 7.0, 3.6, and 1.8 ms, suggesting that one would expect roughly 5, 7, 11, and 20 structures per time trace (from Re_1 to Re_4), and this is generally confirmed by examination of part a of Figs. 2-5.

Part b of Figs. 2-5 shows the results of averaging the time traces for an entire run. A complete run consists of 24 records (e.g., Fig. 2a) for a total of 98,304 recorded points, or 12,288 per probe. As reported earlier,[18,19,22] the adiabatic flame temperature rise is not achieved in the mean at any location. The mean-temperature profile can be thought of as resulting from a duty cycle[18,19] phenomenon, whereby a given probe spends varying lengths of time, dependent upon its position within the layer, in alternate regions of hot and cool fluid. This results in a lower mean temperature rise toward the outer edges of the layer and a higher mean temperature rise within. In addition, part b of Figs. 2-5 shows the highest and lowest temperatures recorded by each probe during the course of a run. It is clear that the layer can be quite hot across its entire width (owing to the passage of a large structure) or quite cool across its entire width (owing to the presence of the cool fluid tongues). It must be noted that none of the data shown here are compensated for the thermal lag and conduction error of the wire (which we believe cannot be estimated without independent knowledge of the instantaneous velocity); but as noted earlier,[18,19] these errors do not affect the mean-temperature profile.

Finally, Fig. 6 shows the mean-temperature profiles for the three lowest Reynolds numbers investigated. The distance to the virtual origin $(x-x_0)$ is taken to be the same for all runs, so that some of the increase in width at Re_1 may be related to a change in x_0. There appears a modest decrease in maximum mean temperature from Re_2 to Re_1. This may be related to the fact that our measuring station at Re_1 is closer (and thus more sensitive) to the mixing transition than at the other Reynolds numbers. We believe these flows to be fully developed, since at Re_2 the measuring station is about 2800 initial high-speed boundary-layer momentum thicknesses downstream, with this value increasing for higher Re and decreasing for lower Re. Above Re_2 there appears to be a modest decrease in the mean-temperature profile, with the width of the layer remaining essentially unchanged. It is also important to note that decreasing the chemical time by using 50% more NO at Re_2 and Re_3 produced no significant difference in the mean-temperature profiles, suggesting that the chemistry is sufficiently fast for the runs reported here.

In order to investigate the effects of Reynolds number further, the high-speed boundary layer of two of the flows, Re_2 and Re_3, were tripped by placing a 0.75-mm-diam rod 5 cm upstream of the splitter plate trailing edge. The Reynolds numbers associated with these flows are designated Re_{2T} and Re_{3T}, respectively. At Re_{2T} the trip was about $5\theta_1$ in height,

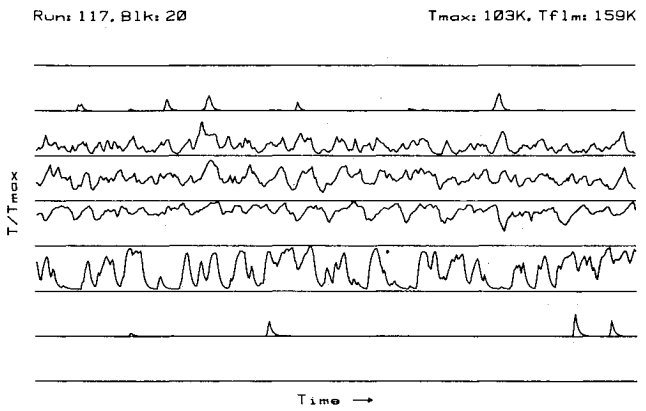

Fig. 5a Temperature vs time trace, Re_4.

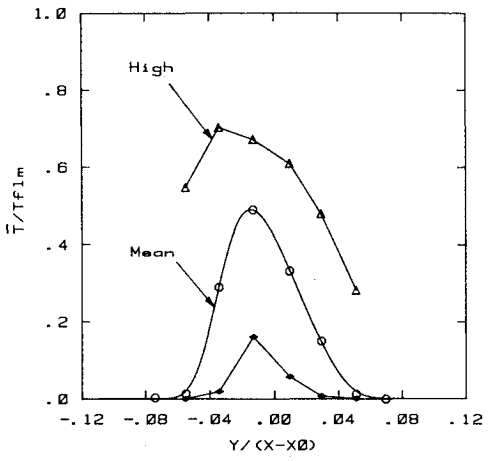

Fig. 5b Mean-temperature profile, Re_4.

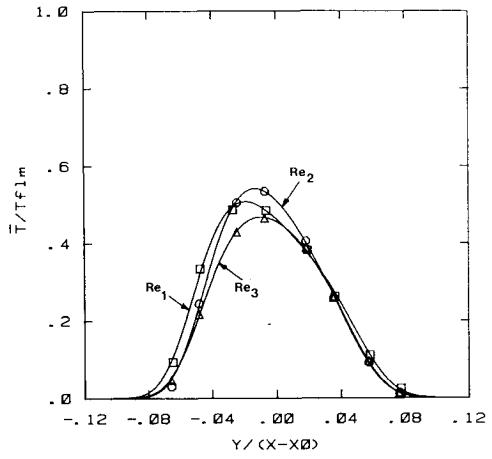

Fig. 6 Mean-temperature profiles, Re_1, Re_2, Re_3.

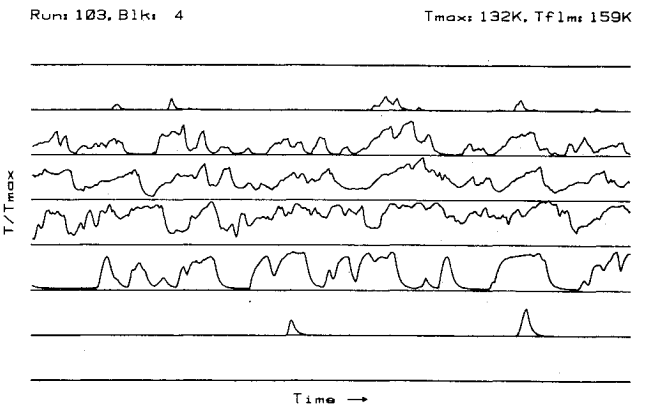

Fig. 7a Temperature vs time trace, Re_{2T}.

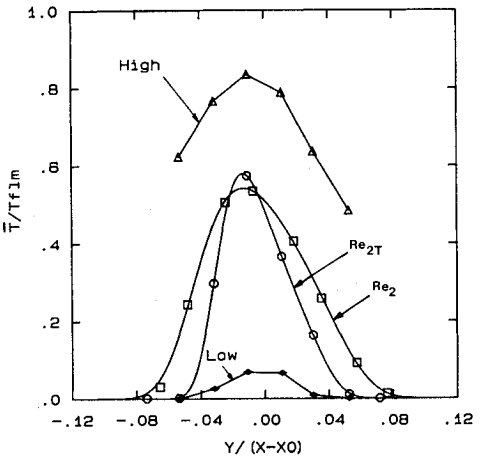

Fig. 7b Mean-temperature profiles, Re_2, Re_{2T}.

Table 1 Summary of results

Run	$\bar{T}$max / Tflm	$\delta_1/(x-x_0)$	Area	δ_{P2}/δ_1	Re
Re_1	0.508	0.172	0.0456	0.236	4.25×10^4
Re_2	0.542	0.162	0.0438	0.240	6.67×10^4
Re_3	0.467	0.165	0.0399	0.215	1.33×10^5
Re_{2T}	0.579	0.109	0.0297	0.243	4.49×10^4
Re_{3T}	0.508	0.116	0.0278	0.213	9.33×10^4
Re_4	0.490	0.120	0.0278	0.206	1.87×10^5

N. B.: Tflm is the adiabatic flame temperature rise, = 158.7 K; $\bar{T}$max the maximum value of $\bar{T}$; δ_1 the width of the layer where $\bar{T}=1\%$ of $\bar{T}$max; Area $\equiv(1/T\text{flm})\int\bar{T}d\eta$; $\eta\equiv y/(x-x_0)$; $x-x_0=45.7$ cm for all runs.

and $300\theta_1$ upstream of the splitter tip, where θ_1 is the momentum thickness of the undisturbed high-speed boundary layer at the splitter tip, estimated using Thwaites' method. These trip conditions are similar to those of Browand and Latigo.[6] The time traces and mean temperature profile for Re_{2T} are shown in Fig. 7, while similar results are shown in Fig. 8 for Re_{3T}, together with a comparison of the untripped data. The most dramatic result is the significant thinning of the layer (by about 30%), with a corresponding reduction in the area under the mean profile. There is a slight increase (7-8%) in the maximum mean temperature in both cases. It is interesting that for both the tripped and untripped cases the area under the mean profile divided by the 1% thickness is essentially unchanged. There is, however, a decrease with increasing Reynolds number.

Browand and Latigo[6] reported that mean profiles of velocity and other turbulence quantities such as the Reynolds stress become self-similar for both tripped and untripped flows if the transverse coordinate utilized is y/θ instead of the usual $y/(x-x_0)$, where θ is the integral thickness of the layer. Presumably the same would hold for this flow, even though the mean-temperature profiles do show a small difference in height that would contradict the assumption of self-similarity between the tripped and untripped flow. It is interesting to note that Koochesfahani,[17] in a study of mixing and product formation in a liquid mixing layer for the $\phi=10$ case, also found that the width of the mixing layer decreased significantly and the height of the mean product profile increased slightly when the layer had tripped naturally with increasing speed.

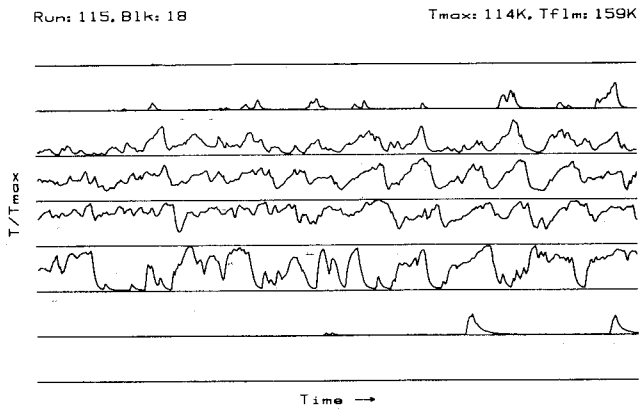

Fig. 8a Temperature vs time trace, Re_{3T}.

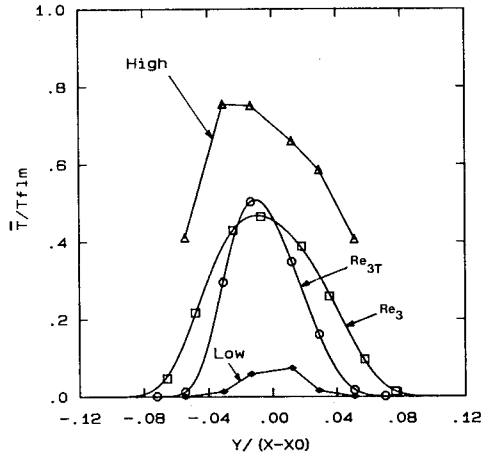

Fig. 8b Mean-temperature profiles, Re_3, Re_{3T}.

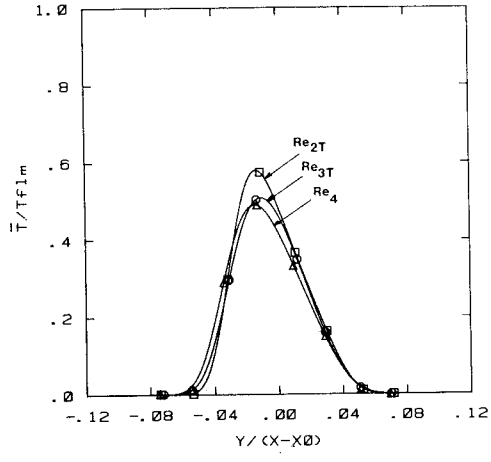

Fig. 9 Mean-temperature profiles, Re_{2T}, Re_{3T}, Re_4.

Figure 9 shows the mean profiles of the tripped layers Re_{2T} and Re_{3T} and the naturally tripped flow Re_4. There appears to be a modest decrease in maximum mean temperature with increasing speed, suggesting a contradiction with the Reynolds number similarity hypothesis.

Figure 10 shows schlieren photographs of the first 25 cm of the layer, at Re_2, Re_{2T}, and Re_4. In spite of the optical integration across the span of the layer, the large structure organization of the flow is readily apparent, in agreement with several earlier works.[2,4,7,9-11,14,16,17,21,22] These (and other) photographs confirm the flow structure already shown in the time traces. The decreased linear growth rate of the tripped layer is evident in comparison with the untripped layer. The visual

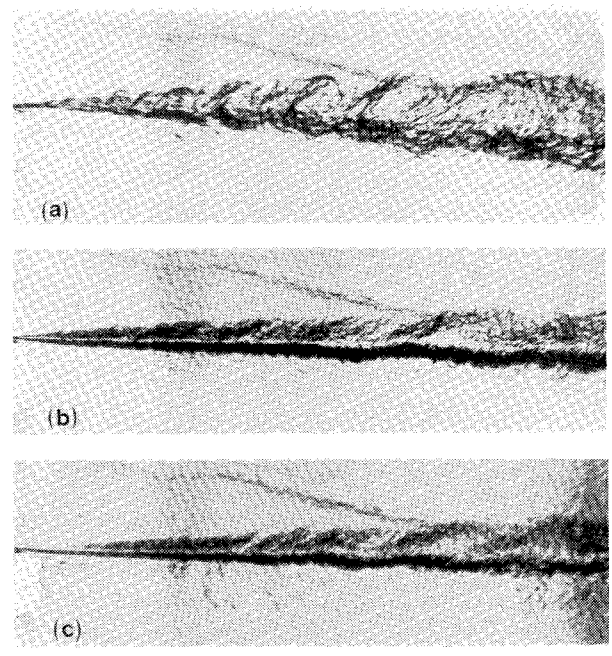

Fig. 10 Mixing layer, a) Re_2, b) Re_{2T}, c) Re_4.

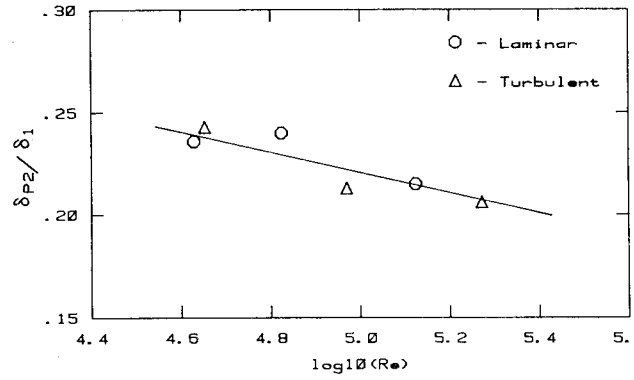

Fig. 11 Product thickness vs log $_{10}Re$.

thickness of the layer, δ_{vis}, obtained from such photographs is in good agreement with the values quoted by Brown and Roshko[7] for untripped layers, and agrees well with the 1% thickness, δ_1.

In order to determine whether Reynolds number plays a role in mixing, the results shown above (see also Table 1) have been plotted in Fig. 11. The ordinate shows the product thickness, δ_{P2}, normalized by the 1% thickness, δ_1. The product thickness[4,16-19] is defined as

$$\delta_{P2} = \int \frac{c_p(y)}{c_{02}} dy$$

where $c_p(y)$ is the concentration of product across the layer and c_{02} is the low-speed freestream molar concentration. Since product is analogous to temperature rise, the product thickness is obtained from the measured mean-temperature profile $\bar{T}(y)$, the molar heat capacity of the carrier gas C_p, and the heat release per mole of reactant ΔQ, i.e.,

$$\delta_{P2} = \int \frac{C_p \bar{T}(y)}{c_{02} \Delta Q} dy$$

The abscissa shows the logarithm (base 10) of the Reynolds number based on velocity difference and 1% thickness. Also shown are the results for the tripped layers. A straight line of

slope 20% per decade (6% per factor of 2) has been faired through all points. There is some question about whether the tripped and untripped results should be considered on the same plot, but, in any event, a decreasing trend is suggested. This implies that for a turbulent mixing layer sufficiently past the mixing transition, and in the limit of fast chemistry, the mean-temperature profile would not be self-similar, since the peak of this profile would decrease with increasing downstream distance (or Reynolds number). One may legitimately suggest that the effects measured here are merely Damkohler number effects, but as mentioned earlier the chemistry can be taken to be fast for all speeds, so we conclude that the bulk of the measured decrease is fluid mechanical and not a result of slow chemistry.

Bradshaw[3] has discussed the effects of initial conditions and virtual origin upon the development of free shear layers that may lead to spurious Reynolds number effects (see also Ho and Huerre[13] and Hussain[14]). While the results presented here may be affected by both the virtual origin and closeness to the mixing transition at Re_1, we anticipate less of a problem at the higher Reynolds numbers. This issue, however, is a difficult one and illustrates the overall problem in making a definitive statement about the effects of Reynolds number.

The recent theoretical model of Broadwell and Breidenthal[5] suggests that Reynolds and Schmidt numbers play similar roles with respect to mixing. As discussed earlier, in this model the amount of product contained in the turbulent mixing layer is divided into a Reynolds number independent part and a Reynolds number dependent part, with current best estimates[17] suggesting that these amounts are roughly equal at Re_2. The model predicts a dependence on Reynolds number that is algebraic rather than logarithmic as reported here. Note that while this dependence is expected for the mean-product profile in a reacting flow, the model predicts self-similarity for the mean profile of a passive scalar, such as heat, as has been measured by Fiedler.[10]

Finally, it must be pointed out that if a weak Reynolds number dependence exists in the limit of fast chemistry, then this implies that the probability density function of the mixture fraction[16-18,22] must also be a weak function of Reynolds number. This would be the case, since in the limit of fast chemistry the mean-temperature profile is computed from the probability density function and a weighting function determined by the equivalence ratio ϕ (see discussion in Appendix of Ref. 18).

Conclusions

Results presented here suggest that the processes of mixing and entrainment in a two-dimensional turbulent mixing layer are dominated by the dynamics of the large scale structures, over a wide range of Reynolds numbers. The results also suggest that the mean-temperature profile, in the limit of fast chemistry, is not self-similar, owing to a modest decrease in mean temperature rise with increasing Reynolds number. It is also found that tripping the high-speed boundary layer produces a significant thinning of the layer and a slight increase in maximum mean temperature, suggesting that the flow is not self-similar under trip/no-trip conditions. It is believed that tripping the layer should provide a good test of current computational models in their ability to incorporate the effects of initial conditions.

Acknowledgments

We would like to acknowledge the many helpful discussions with Dr. J. E. Broadwell during the course of the research reported here, the assistance of Mr. C. E. Frieler, as well as the expert help of Mr. Earl Dahl throughout. This work was sponsored by the Air Force Office of Scientific Research, Contract F49620-79-C-0159.

References

[1]Batt, R. G., "Some Measurements on the Effect of Tripping the Two-Dimensional Shear Layer," *AIAA Journal,* Vol. 13, 1975, pp. 245-247.

[2]Bernal, L. P., "The Coherent Structure of Turbulent Mixing Layers: I. Similarity of the Primary Vortex Structure. II. Secondary Streamwise Vortex Structure," Ph.D. Thesis, California Institute of Technology, 1981.

[3]Bradshaw, P., "The Effect of Initial Conditions on the Development of a Free Shear Layer," *Journal of Fluid Mechanics,* Vol. 26, No. 2, 1966, pp. 225-236.

[4]Breidenthal, R. E., "A Chemically Reacting, Turbulent Shear Layer," Ph.D. Thesis, California Institute of Technology, 1978; also, "Structure in Turbulent Mixing Layers and Wakes Using a Chemical Reaction," *Journal of Fluid Mechanics,* Vol. 109, 1981, pp. 1-24.

[5]Broadwell, J. E. and Breidenthal, R. E., "A Simple Model of Mixing and Chemical Reaction in a Turbulent Shear Layer," *Journal of Fluid Mechanics,* Vol. 125, 1982, pp. 397-410.

[6]Browand, F. K. and Latigo, B. O., "Growth of the Two-Dimensional Mixing Layer from a Turbulent and Non-Turbulent Boundary Layer," *The Physics of Fluids,* Vol. 22, No. 6, 1979, pp. 1011-1019.

[7]Brown, G. L. and Roshko, A., "On Density Effects and Large Structure in Turbulent Mixing Layers," *Journal of Fluid Mechanics,* Vol. 64, No. 4, 1974, pp. 775-816.

[8]Cohen, N. and Bott, J. F., "Review of Rate Data for Reactions of Interest in HF and DF Lasers," The Aerospace Corp., Calif., Rept. SD-TR-82-86, 1982.

[9]Dimotakis, P. E. and Brown, G. L., "The Mixing Layer at High Reynolds Number: Large Structure Dynamics and Entrainment," *Journal of Fluid Mechanics,* Vol. 78, No. 3, 1976, pp. 535-560.

[10]Fiedler, H. F., "On Turbulent Structure and Mixing Mechanisms in Free Turbulent Shear Flows," *Turbulent Mixing in Nonreactive and Reactive Flows, A Project SQUID Workshop,* Plenum Press, New York, 1975, pp. 381-410.

[11]Ganji, A. T. and Sawyer, R. F., "Turbulence, Combustion, Pollutant, and Stability Characterization of a Premixed, Step Combustor," NASA CR 3230, 1980; also, "Experimental Study of the Flowfield of a Two-Dimensional Premixed Turbulent Flame," *AIAA Journal,* Vol. 18, July 1980, pp. 817-824.

[12]Hermanson, J. C., Mungal, M. G., and Dimotakis, P. E., "Heat Release Effects on Shear Layer Growth and Entrainment," AIAA Paper 85-0142, Jan. 1985.

[13]Ho, C-M. and Huerre, P., "Perturbed Free Shear Layers," *Annual Review of Fluid Mechanics,* Vol. 16, 1984, pp. 365-425.

[14]Hussain, A. K. M. F., "Coherent Structures—Reality and Myth," *The Physics of Fluids,* Vol. 26, No. 10, 1983, pp. 2816-2850.

[15]Kee, R. J., Miller, J. A., and Jefferson, T. H., "CHEMKIN: A General-Purpose, Problem-Independent, Transportable, Fortran Chemical Kinetics Code Package," Sandia Labs., Livermore, Calif., Rept. SAND80-8003, 1980.

[16]Konrad, J. H., "An Experimental Investigation of Mixing in Two-Dimensional Turbulent Shear Flows with Application to Diffusion-Limited Chemical Reactions," Ph.D. Thesis, California Institute of Technology, 1976; also, Project SQUID Tech. Rept. CIT-8-PU, 1976.

[17]Koochesfahani, M. M., "Experiments on Turbulent Mixing and Chemical Reactions in a Liquid Mixing Layer," Ph.D. Thesis, California Institute of Technology, 1984.

[18]Mungal, M. G. and Dimotakis, P. E., "Mixing and Combustion with Low Heat Release in a Turbulent Shear Layer," *Journal of Fluid Mechanics,* Vol. 148, 1984, pp. 349-382.

[19]Mungal, M. G., Dimotakis, P. E., and Broadwell, J. E., "Turbulent Mixing and Combustion in a Reacting Shear Layer," *AIAA Journal,* Vol. 22, June 1984, pp. 797-800.

[20]Paranthoen, P., Petit, C., and Lecordier, J. C., "The Effect of the Thermal Prong-Wire Interaction on the Response of a Cold Wire in Gaseous Flows (Air, Argon and Helium)," *Journal of Fluid Mechanics,* Vol. 124, 1982, pp. 457-473.

[21]Winant, C. D. and Browand, F. K., "Vortex Pairing: The Mechanism of Turbulent Mixing-Layer Growth at Moderate Reynolds Number," *Journal of Fluid Mechanics,* Vol. 63, No. 2, 1974, pp. 237-255.

[22]Wallace, A. K., "Experimental Investigation of the Effects of Chemical Heat Release in the Reacting Turbulent Plane Shear Layer," Ph.D. Thesis, The University of Adelaide, 1981; also, Rept. AFOSR-TR-84-0650, 1984.